

Quantum Lifshitz points in an altermagnetic metal

Hui Hu¹ and Xia-Ji Liu¹

¹Centre for Quantum Technology Theory, Swinburne University of Technology, Melbourne 3122, Australia

(Dated: May 16, 2025)

We predict the existence of two tri-critical quantum Lifshitz points in recently discovered d -wave altermagnetic metals subjected to an external magnetic field. These points connect a spatially modulated Fulde–Ferrell–Larkin–Ovchinnikov (FFLO) phase, a uniform polarized Bardeen–Cooper–Schrieffer (BCS) superconducting phase, and the normal metallic phase in a nontrivial manner. Depending on whether the FFLO state is primarily induced by the magnetic field or by d -wave altermagnetism, we classify the corresponding Lifshitz points as field-driven or altermagnetism-driven, respectively. Notably, the two types exhibit distinct behaviors: the transition from the FFLO phase to the polarized BCS phase is first-order near the field-driven Lifshitz point, as might be expected, whereas it becomes continuous near the altermagnetism-driven Lifshitz point. We further explore the effects of finite temperature and find that the altermagnetism-driven Lifshitz point is significantly more sensitive to thermal fluctuations.

Understanding phase transitions between different competing quantum orders lies at the heart of diverse fields [1, 2], including quantum many-body physics, condensed matter physics, and high-energy particle physics. In this regard, a special critical point known as the tri-critical Lifshitz point attracts specific attention over the last several decades, due to its unusual critical exponents [3–7]. The Lifshitz point arises when three phases meet together: two ordered phases (one uniform and another unevenly distributed in real space) coexisting with a disordered phase. Typically, Lifshitz points are classical and present at nonzero temperature ($T > 0$), where the disordered to ordered transitions are often driven by thermal fluctuations [3]. The most known examples include helimagnetic materials such as MnP nanorod films [8], inhomogeneous polymers [9, 10], ferroelectric chiral smectic liquid crystals [11], spin-population imbalanced Fermi gases [12], and even hot dense quantum chromodynamics (QCD) matters [7, 13].

In principle, the Lifshitz point can also emerge at zero temperature ($T = 0$) [14], where phase transitions are governed solely by quantum fluctuations [1]. Nonetheless, identifying such a *quantum* Lifshitz point in real materials has proven to be exceptionally challenging. To date, theoretical studies of quantum Lifshitz points have primarily focused on some idealized models or systems, such as the infinite-dimensional Hubbard model [15], the frustrated ferromagnetic Heisenberg chain [16], the two-dimensional (2D) effective theory with specifically engineered interaction potential [17], the spin-1/2 square-lattice $J - Q$ model [18], the frustrated 2D XY model [19], and Fermi mixtures with both spin-imbalance and mass-imbalance [20].

In this Letter, we would like to propose that, the recently discovered *altermagnetic* metals may provide an ideal avenue to realize and observe the long-sought quantum Lifshitz point and to explore its unconventional critical exponents. Altermagnetism represents a distinct form of magnetic order, different from the well-known ferro-

magnetism and antiferromagnetism [21–26]. In altermagnetic metals, collinear spin arrangements result in zero net magnetization; however, due to specific crystal symmetries, significant spin splitting still appears in the electronic band structure. This unique spin-splitting behavior can have profound effects when inter-particle interactions are considered [27–29]. Of particular relevance to our study is the recent surprising discovery [30, 31] of an altermagnetism-induced spatially inhomogeneous Fulde–Ferrell–Larkin–Ovchinnikov (FFLO) phase [32, 33] under attractive interactions.

Here, we compare the FFLO state induced by altermagnetism [30, 31] with the conventional FFLO state driven by an external magnetic field [32–38]. Surprisingly, we discover that altermagnetism and the magnetic field actually compete with one another in promoting the spatially modulated superconducting FFLO phase. This competition gives rise to a homogeneous, spin-population-polarized Bardeen–Cooper–Schrieffer (BCS) phase, emerging from their combined influence. This newly identified polarized BCS phase represents a uniform ordered state, whereas the two FFLO phases — one arising from altermagnetism and the other from a magnetic field — constitute exotic ordered states characterized by broken spatial uniformity. Furthermore, recognizing that a disordered normal state inevitably appears under sufficiently strong altermagnetism or magnetic field, even at zero temperature, we identify the presence of two quantum Lifshitz points. Remarkably, these arise naturally without requiring fine-tuning of system parameters such as the mass imbalance or the specific form of the interaction potential.

The emergence of quantum Lifshitz points in altermagnetic metals offers a rare opportunity to deepen our understanding of the unusual universal critical exponents characteristic of the Lifshitz regime [3–6], where quantum fluctuations are expected to play a pivotal role [7]. At the mean-field level, we already distinguish the distinct nature of the two predicted quantum Lifshitz points, as the

phase transition between the two ordered superconducting states exhibits different behaviors — one being a discontinuous first-order transition and the other a smooth second-order transition. We hypothesize that these quantum Lifshitz points may remain robust in the presence of quantum fluctuations, a question that calls for more comprehensive theoretical exploration. We also anticipate that future experiments will uncover the intriguing and anomalous quantum critical phenomena associated with these transitions.

Model. – We consider a 2D spin-1/2 interacting Fermi system with d -wave altermagnetism in a unit area subjected to an external magnetic field h , as described by a Hamiltonian density ($s_\uparrow = +1$ and $s_\downarrow = -1$),

$$\mathcal{H} = \sum_{\sigma=\uparrow,\downarrow} \psi_\sigma^\dagger \left[\hat{\xi}_{\mathbf{k}} + s_\sigma (\hat{J}_{\mathbf{k}} + h) \right] \psi_\sigma^\dagger + U_0 \psi_\uparrow^\dagger \psi_\downarrow^\dagger \psi_\downarrow \psi_\uparrow, \quad (1)$$

where $\psi_\sigma(\mathbf{x})$ is the annihilation field operator for a fermion in the spin state σ , $\hat{J}_{\mathbf{k}} = \lambda \hbar^2 \hat{k}_x \hat{k}_y / (2m)$ with $\hat{k}_{x,y} \equiv -i\partial_{x,y}$ and the dimensionless coupling constant λ is the spin-splitting due to the d -wave altermagnetism [22, 31] and $\hat{\xi}_{\mathbf{k}} = -\hbar^2 \nabla^2 / (2m) - \mu$ is the conventional dispersion relation, with chemical potential μ that fixes the average density n . For simplicity, we consider an s -wave attractive contact interaction, with its strength $U_0 = -\sum_{\mathbf{k}} 1 / [\hbar^2 k^2 / m + \varepsilon_B] < 0$ characterized by a two-body binding energy ε_B [39]. Hereafter, the wavevector k and energy (such as h and ε_B) are measured in units of the Fermi wavevector $k_F = (2\pi n)^{1/2}$ and Fermi energy $\varepsilon_F = \hbar^2 k_F^2 / (2m) = k_B T_F$, respectively. Throughout the paper, we take a binding energy $\varepsilon_B = 0.08\varepsilon_F$.

Pairing instability. – At sufficiently low temperature, the attractive interaction drives the spin-1/2 Fermi system into a superconducting state. This pairing instability is mostly easily seen by introducing a pairing field $\Delta(\mathbf{x}, \tau)$ through the standard Hubbard-Stratonovich transformation, which couples to $\psi_\uparrow^\dagger \psi_\downarrow^\dagger$ [39, 40]. By integrating out the fermionic field operators and truncating to fourth order in the pairing field $\Delta(Q \equiv \{\mathbf{q}, i\omega_m\})$ in momentum space, where $\omega_m \equiv 2m\pi k_B T$ with integer $m = 0, \pm 1, \dots$ is the bosonic Matsubara frequency, we obtain [40],

$$\mathcal{S}_{\text{eff}} = \sum_Q \frac{\bar{\Delta}_Q \Delta_Q}{-\Gamma(Q)} + \sum_{Q_1 Q_2 Q_3} \frac{u_{1,2,3}}{2} \Delta_1 \bar{\Delta}_2 \Delta_3 \bar{\Delta}_{1+2-3}. \quad (2)$$

Here, $\bar{\Delta}_{1+2-3}$ is an abbreviation of $\bar{\Delta}(Q_1 + Q_2 - Q_3)$ and the sum \sum_Q stands for $k_B T \sum_m \int d\mathbf{q} / (2\pi)^2$. The inverse vertex function $\Gamma^{-1}(Q) = U_0^{-1} + \chi_{\text{pair}}^0(Q)$ can be calculated by summing all the ladder diagrams for the pair propagator $\chi_{\text{pair}}^0(Q)$ [40],

$$\Gamma^{-1}(Q) = \frac{1}{U_0} + \sum_{\mathbf{k}} \frac{f(\xi_{\mathbf{q}/2+\mathbf{k}\uparrow}) + f(\xi_{\mathbf{q}/2-\mathbf{k}\downarrow}) - 1}{i\omega_m - (\xi_{\mathbf{q}/2+\mathbf{k}\uparrow} + \xi_{\mathbf{q}/2-\mathbf{k}\downarrow})}, \quad (3)$$

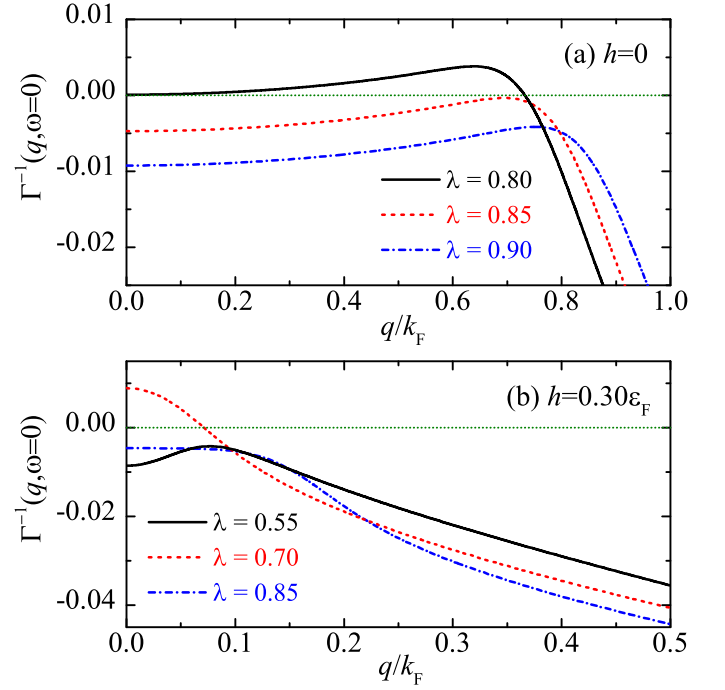


FIG. 1. The pairing momentum q -dependence of the inverse vertex function at zero frequency $\Gamma^{-1}(q, \omega = 0)$, in units of $2m/\hbar^2$, at different altermagnetic couplings λ as indicated, and at the magnetic field $h = 0$ (a) and $h = 0.3\varepsilon_F$ (b). We have taken a negligible temperature $T = 0.01T_F$ to smooth the sharp Fermi surface and to increase numerical accuracy.

where $\xi_{\mathbf{k}\uparrow} = \xi_{\mathbf{k}} + J_{\mathbf{k}} + h$ and $\xi_{\mathbf{k}\downarrow} = \xi_{\mathbf{k}} - J_{\mathbf{k}} - h$, and $f(E) \equiv (e^{E/k_B T} + 1)^{-1}$ is the Fermi-Dirac distribution function. The quartic term in Eq. (2) represents an effective repulsion between Cooper pairs at the lowest order [39, 40]. In this Born approximation, it suffices to suppress the momentum dependence of the coefficient $u_{1,2,3}$ [39, 40]: $u \equiv u(Q_1 = 0, Q_2 = 0, Q_3 = 0) = \sum_K G_{0\uparrow}^2(K) G_{0\downarrow}^2(-K) > 0$, where $G_{0\sigma}(K)$ is the non-interacting Green function of fermions at the four-momentum $K \equiv \{\mathbf{k}, i\omega_n\}$.

The superconducting instability is determined by the well-known Thouless criterion ($i\omega_m \rightarrow \omega + i0^+$),

$$\max_{\{\mathbf{q}\}} \Gamma^{-1}(\mathbf{q}, \omega = 0) |_{T=T_c} = 0, \quad (4)$$

generalized here to allow a nonzero center-of-mass momentum $\mathbf{q} \neq 0$ of Cooper pairs, which signals a spatially inhomogeneous FFLO superconducting state [41]. In Fig. 1, we report the q -dependence of the inverse vertex function $\Gamma^{-1}(q = |\mathbf{q}|, \omega = 0)$, with varying altermagnetic coupling λ at the two magnetic fields, $h = 0$ (a) and $h = 0.3\varepsilon_F$ (b), and at essentially zero temperature $T = 0.01T_F$. At zero magnetic field in Fig. 1(a), the maximum of $\Gamma^{-1}(q, \omega = 0)$ always occurs at a finite momentum $q_{\text{max}} \neq 0$ and becomes non-negative once $\lambda \geq \lambda_c \simeq 0.85$, indicating the onset of an altermagnetism-induced FFLO state. This result aligns with previous

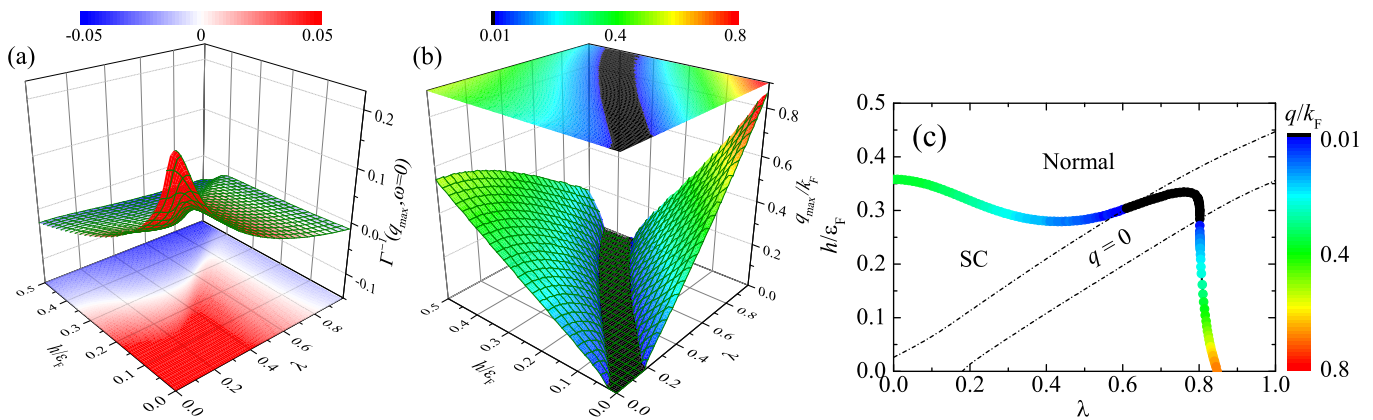


FIG. 2. (a) The maximum of the inverse vertex function $\Gamma^{-1}(q_{\max}, \omega = 0)$, as functions of the altermagnetic coupling λ and magnetic field h/ε_F . (b) The corresponding pairing momentum q_{\max} . (c) The instability line determined by the Thouless criterion $\Gamma^{-1} = 0$ separates the superconducting phase (SC) from the normal state. The color of the line shows the pairing momentum. The pairing momentum is identically zero between the two dot-dashed lines.

mean-field calculations [30, 31], despite differences in the model Hamiltonians and interaction types employed. In stark contrast, at a finite magnetic field $h = 0.3\varepsilon_F$ as shown in Fig. 1(b), the position of the maximum q_{\max} exhibits a non-monotonic dependence on increasing λ . While the inverse vertex function reaches its maximum at a nonzero momentum q_{\max} for both relatively weak and strong altermagnetic couplings, it peaks precisely at zero momentum when $\lambda = 0.70$. This suggests that, at this intermediate coupling constant, the system favors a BCS-like superconducting state that is spatially uniform.

Quantum Lifshitz points. – To understand this non-monotonic behavior, it is instructive to Taylor-expand the inverse vertex function, keeping the leading orders in powers of q and ω , i.e., $-\Gamma^{-1}(q, \omega) = r + Zq^2 + Dq^4 - \gamma\omega$, where the expansion coefficients $\{Z, D > 0, \gamma > 0\}$ as well as $r = -\Gamma^{-1}(0, 0)$ are functions of the altermagnetic coupling λ and magnetic field h . Therefore, we may directly write down a Ginzburg-Landau (GL) Lagrangian at the low-energy from \mathcal{S}_{eff} in Eq. (2),

$$\mathcal{L} = \gamma \bar{\Delta} \partial_\tau \Delta + Z |\partial_x \Delta|^2 + D |\partial_x^2 \Delta|^2 + r |\Delta|^2 + \frac{u}{2} |\Delta|^4. \quad (5)$$

Physically, the expansion coefficient $Z(\lambda, h)$ presents the (inverse) mass of Cooper pairs. A superconducting transition takes place when the global minimum of the action $\mathcal{S}_{\text{GL}} = \int dx d\tau \mathcal{L}[\Delta(\mathbf{x}, \tau)]$ is located at a nonzero pairing field $\langle \Delta(\mathbf{x}, \tau) \rangle \neq 0$, which describes a condensate of pairs. When $Z(\lambda, h)$ is negative, Cooper pairs of the lowest energy would have a finite momentum $q_0 = \sqrt{-Z/(2D)}$, in order to minimize the combined gradient (kinetic energy) term, $Zq^2 + Dq^4$ [7]. As a result, the parameter r effectively renormalizes to $\bar{r} = r - Z^2/(4D)$ and a second-order transition occurs at a critical altermagnetic coupling λ_c determined by $\bar{r}(h, \lambda_c) = 0$ for a fixed magnetic field h . This mechanism underlies the onset of the altermagnetism-induced FFLO state illustrated in Fig.

1(a). Conversely, when $Z(\lambda, h)$ is positive, the pairs have the lowest energy at zero momentum $q_0 = 0$. In this case, a uniform superconducting state emerges as the pairing field Δ becomes constant, with the transition occurring at $r(h, \lambda_c) = 0$. This behavior corresponds to the BCS-like state observed at $\lambda = 0.70$ in Fig. 1(b). However, an interesting question arises: why does a nonzero q_{\max} appear when λ is increased or decreased from 0.70, suggesting negative Z ? A simple explanation is that the coefficient $Z(h, \lambda)$ may change sign as a function of λ , thereby altering the momentum structure of the lowest-energy Cooper pairs.

This leads to an intriguing possibility: by appropriately tuning h and λ , both coefficients $r(h, \lambda)$ and $Z(h, \lambda)$ might simultaneously vanish at certain tri-critical Lifshitz points $(h_{\text{LFP}}, \lambda_{\text{LFP}})$, at which two ordered phases (i.e., the FFLO state and BCS-like state) merge with a disordered, normal phase. To confirm such an anticipation, we present contour plots in Fig. 2(a) and Fig. 2(b), which show the maximum of the inverse vertex function $\Gamma^{-1}(q_{\max}, \omega = 0)$ and the corresponding pair momentum q_{\max} in the λ - h plane, respectively. In the context of our low-energy GL theory, the former serves as a proxy for the coefficient $-r$ (or $-\bar{r}$), while the latter can be interpreted as q_0 . Remarkably, Fig. 2(b) reveals a dark stripe, indicating a region where the pairing momentum is strictly zero. Fig. 2(c) outlines the boundaries of this stripe using two dot-dashed lines and includes an instability line determined by the Thouless criterion. These dot-dashed lines and the instability line correspond to the conditions $Z = 0$ and $r = 0$ (or $\bar{r} = 0$), respectively. Their intersections mark the anticipated tri-critical Lifshitz points. In Fig. 3, we highlight the two resulting Lifshitz points with orange and purple dots.

It is worth noting that the two predicted Lifshitz points are quantum critical points [1], as our analysis is conducted at essentially zero temperature. In contrast, most

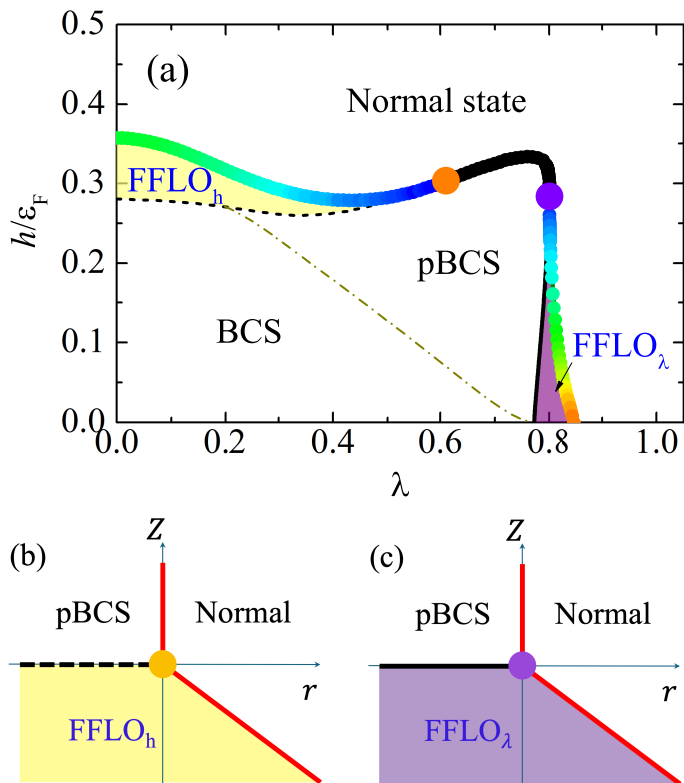


FIG. 3. (a) The phase diagram determined by the mean-field calculations, which further reveal the existence of the standard BCS phase, a polarized BCS phase and two FFLO states inside the superconducting phase. This leads to two quantum Lifshitz points, as highlighted by the orange and purple dots, respectively. (b) and (c) A sketch of phase diagrams near the quantum Lifshitz points, constructed by using the phenomenological parameters Z and r following the effective action. The solid lines and dashed lines in the phase diagrams correspond to the second-order and first-order phase transitions, respectively.

previous studies focus on classical Lifshitz points, where tuning the temperature is typically required to drive the Cooper-pair mass Z to zero or negative values ($Z \leq 0$) [12]. In such cases, the transition to an ordered phase is governed by thermal fluctuations. Even when a quantum Lifshitz point emerges accidentally at zero temperature, the two ordered phases are generally separated by a finite-temperature quantum critical regime [14]. In our case, however, the predicted quantum Lifshitz points are driven purely by quantum fluctuations, and the two superconducting ordered states are directly connected in the phase diagram. This makes the altermagnetic metal a particular promising platform for probing the rich quantum nature of Lifshitz points. For instance, the dynamic exponent $z = 4$ becomes large precisely at the quantum Lifshitz point, rendering the associated critical exponents very unusual. A detailed analysis of these critical exponents, within the framework of the Hertz-Millis theory [42, 43] will be presented in future work.

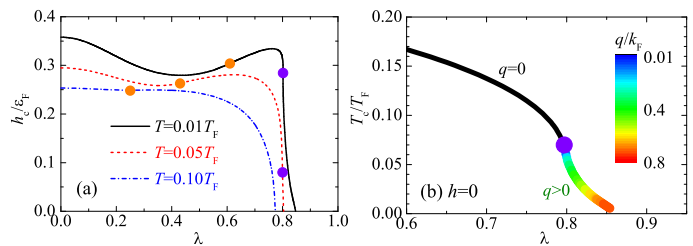


FIG. 4. (a) The instability lines at three temperatures $T/T_F = 0.01, 0.05$ and 0.10 , with the Lifshitz points highlighted by dots. (b) The critical temperature T_c as a function of the altermagnetic coupling λ at zero magnetic field $h = 0$. The color of the line shows the pairing momentum at the phase transition. The purple dot indicates the zero-field Lifshitz point at $\lambda \simeq 0.8$ and at $T \simeq 0.07T_F$.

Two types of quantum Lifshitz points. – Thus far, our analysis has been limited to the normal state, as we assumed the smallness of the pairing field in deriving the effective action \mathcal{S}_{eff} in Eq. (2). To explore the superconducting phases, we have also applied the mean-field theory to calculate the nonzero order parameter $\Delta(\mathbf{x})$, as detailed in a companion paper [44]. The resulting phase diagram is presented in Fig. 3(a), which clearly distinguishes between different FFLO states induced by either the external magnetic field or the intrinsic altermagnetism. These two mechanisms of FFLO formation compete, ultimately giving rise to the dark stripe of zero pairing momentum identified in Fig. 2(c). Interestingly, beyond the superfluid transition, the BCS-like superconducting phase manifests as a novel polarized BCS state characterized by an imbalance in spin population [44].

The two predicted quantum Lifshitz points are distinct, as the nature of the phase transitions between the polarized BCS state and the two FFLO states differs significantly. For the field-induced FFLO state (i.e., FFLO_h), the transition to the polarized BCS state is first-order. In contrast, the transition from the altermagnetism-driven FFLO state (i.e., FFLO_λ) to the polarized BCS state is continuous. We tentatively attribute the discontinuous transition near the magnetic-field-induced quantum Lifshitz point (indicated by the orange dot) to the sign change in the quartic coefficient u , as well as the influence of high-order terms in $|\Delta|^2$ in the GL Lagrangian when extended to the superfluid phase.

Thermal effect on the Lifshitz points. – Finally, we briefly discuss the impact of thermal fluctuations on the Lifshitz points, as illustrated in Fig. 4. As the temperature increases, the Lifshitz point induced by the magnetic field (or by altermagnetism) shifts toward regions of weaker altermagnetic coupling (or lower magnetic field). Notably, the altermagnetism-driven Lifshitz point is more fragile to temperature changes, and disappears entirely when temperature exceeds approximately

$0.07T_F$ (for the binding energy $\varepsilon_B = 0.08\varepsilon_F$ considered in this work), as shown in Fig. 4(b).

Conclusions. – We conclude by discussing the experimental prospects for realizing the predicted quantum Lifshitz points. It is important to emphasize that our proposed mechanism for generating quantum Lifshitz points in altermagnetic metals is both robust and universal – insensitive to the specific type of altermagnetism or the particular partial-wave character of the interaction driving superconductivity [45]. Experimentally, d -wave altermagnetism has been routinely observed in a variety of materials, with the coupling strength often tunable. However, superconductivity coexisting with altermagnetism has yet to be demonstrated. We expect that such superconductivity may soon be observed in altermagnetic materials featuring strong electron-phonon coupling, which naturally gives rise to a phonon-mediated s -wave attractive interaction. Alternatively, d -wave superconductivity could emerge in systems with strong spin fluctuations [46], particularly in materials with significant on-site electronic repulsion.

Acknowledgments. – This research was supported by the Australian Research Council’s (ARC) Discovery Program, Grants Nos. DP240101590 (H.H.) and DP240100248 (X.-J.L.).

-
- [1] S. Sachdev, *Quantum Phase Transitions* (Cambridge University Press, Cambridge, 1999).
- [2] S. Sachdev, *Quantum Phases of Matter* (Cambridge University Press, New York, 2023).
- [3] R. M. Hornreich, M. Luban, and S. Shtrikman, Critical Behavior at the Onset of \vec{k} -Space Instability on the λ Line, *Phys. Rev. Lett.* **35**, 1678 (1975).
- [4] J. Sak and G. S. Grest, Critical exponents for the Lifshitz point: ε -expansion, *Phys. Rev. B* **17**, 3602 (1978).
- [5] C. Mergulhão, Jr. and C. E. I. Carneiro, Field-theoretic calculation of critical exponents for the Lifshitz point, *Phys. Rev. B* **59**, 13954 (1999).
- [6] H. W. Diehl and M. Shpot, Critical behavior at m -axial Lifshitz points: Field-theory analysis and ε -expansion results, *Phys. Rev. B* **62**, 12338 (2000).
- [7] R. D. Pisarski, V. V. Skokov, and A. M. Tsvelik, A pedagogical introduction to the Lifshitz regime, *Universe* **5**, 48 (2019).
- [8] R. P. Madhugaria, C.-M. Hung, B. Muchharla, A. T. Duong, R. Das, P. T. Huy, S. Cho, S. Witanachchi, H. Srikanth, and M.-H. Phan, Strain-modulated helimagnetism and emergent magnetic phase diagrams in highly crystalline MnP nanorod films, *Phys. Rev. B* **103**, 184423 (2021).
- [9] G. H. Fredrickson and F. S. Bates, Design of Bicontinuous Polymeric Microemulsions. *J. Polym. Sci.* **35**, 2775 (1997).
- [10] B. H. Jones and T. P. Lodge, Nanocasting nanoporous inorganic and organic materials from polymeric bicontinuous microemulsion templates. *Polym. J.* **44**, 131 (2012).
- [11] I. Mušević, B. Žekš, and R. Blinc, Th. Rasing and P. Wyder, Phase Diagram of a Ferroelectric Chiral Smectic Liquid Crystal near the Lifshitz Point, *Phys. Rev. Lett.* **48**, 192 (1982).
- [12] K. B. Gubbels, J. E. Baarsma, and H. T. C. Stoof, Lifshitz Point in the Phase Diagram of Resonantly Interacting ${}^6\text{Li}$ – ${}^{40}\text{K}$ Mixtures, *Phys. Rev. Lett.* **103**, 195301 (2009).
- [13] R. Casalbuoni and G. Nardulli, Inhomogeneous superconductivity in condensed matter and QCD, *Rev. Mod. Phys.* **76**, 263 (2004).
- [14] R. Ramazashvili, Quantum Lifshitz point, *Phys. Rev. B* **60**, 7314 (1999).
- [15] F. Günther, G. Seibold, and J. Lorenzana, Quantum Lifshitz Point in the Infinite-Dimensional Hubbard Model, *Phys. Rev. Lett.* **98**, 176404 (2007).
- [16] L. Balents and O. A. Starykh, Quantum Lifshitz Field Theory of a Frustrated Ferromagnet, *Phys. Rev. Lett.* **116**, 177201 (2016).
- [17] J. Wårdh, B. M. Andersen, and M. Granath, Suppression of superfluid stiffness near a Lifshitz-point instability to finite-momentum superconductivity, *Phys. Rev. B* **98**, 224501 (2018).
- [18] B. Zhao, J. Takahashi, and A. W. Sandvik, Multicritical Deconfined Quantum Criticality and Lifshitz Point of a Helical Valence-Bond Phase, *Phys. Rev. Lett.* **125**, 257204 (2020).
- [19] Y. A. Kharkov, J. Oitmaa, and O. P. Sushkov, Quantum Lifshitz criticality in a frustrated two-dimensional XY model, *Phys. Rev. B* **101**, 035114 (2020).
- [20] P. Zdybel and P. Jakubczyk, Quantum Lifshitz points and fluctuation-induced first-order phase transitions in imbalanced Fermi mixtures, *Phys. Rev. Res.* **2**, 033486 (2020).
- [21] L. Šmejkal, R. González-Hernández, T. Jungwirth, and J. Sinova, Crystal time-reversal symmetry breaking and spontaneous Hall effect in collinear antiferromagnets, *Sci. Adv.* **6**, eaaz8809 (2020).
- [22] L. Šmejkal, J. Sinova, and T. Jungwirth, Emerging Research Landscape of Altermagnetism, *Phys. Rev. X* **12**, 040501 (2022).
- [23] I. I. Mazin, Altermagnetism in MnTe: Origin, predicted manifestations, and routes to detwinning, *Phys. Rev. B* **107**, L100418 (2023).
- [24] P. Das, V. Leeb, J. Knolle, and M. Knap, Realizing Altermagnetism in Fermi-Hubbard Models with Ultracold Atoms, *Phys. Rev. Lett.* **132**, 263402 (2024).
- [25] M. Hiraiishi, H. Okabe, A. Koda, R. Kadono, T. Muroi, D. Hirai, and Z. Hiroi, Nonmagnetic ground state in RuO₂ revealed by muon spin rotation, *Phys. Rev. Lett.* **132**, 166702 (2024).
- [26] O. J. Amin, A. Dal Din, E. Golias, Y. Niu, A. Zakharov, S. C. Fromage, C. J. B. Fields, S. L. Heywood, R. B. Cousins, F. Maccherozzi, J. Krempaský, J. H. Dil, D. Kriegner, B. Kiraly, R. P. Campion, A. W. Rushforth, K. W. Edmonds, S. S. Dhesi, L. Šmejkal, T. Jungwirth, and P. Wadley, Nanoscale imaging and control of altermagnetism in MnTe, *Nature* **636**, 348 (2024).
- [27] P. A. McClarty and J. G. Rau, Landau Theory of Altermagnetism, *Phys. Rev. Lett.* **132**, 176702 (2024).
- [28] Y. Fukaya, B. Lu, K. Yada, Y. Tanaka, and J. Cayao, Superconducting phenomena in systems with unconventional magnets, arXiv:2502.15400 (2025).
- [29] H.-J. Lin, S.-B. Zhang, H.-Z. Lu, and X. C. Xie, Coulomb Drag in Altermagnets, *Phys. Rev. Lett.* **134**, 136301 (2025).

- (2025).
- [30] D. Chakraborty and A. M. Black-Schaffer, Zero-field finite-momentum and field-induced superconductivity in altermagnets, *Phys. Rev. B* **110**, L060508 (2024).
- [31] S. Hong, M. J. Park, and K.-M. Kim, Unconventional p -wave and finite-momentum superconductivity induced by altermagnetism through the formation of Bogoliubov Fermi surface, *Phys. Rev. B* **111**, 054501 (2025).
- [32] P. Fulde and R. A. Ferrell, Superconductivity in a Strong Spin-Exchange Field, *Phys. Rev.* **135**, A550 (1964).
- [33] A. I. Larkin and Yu. N. Ovchinnikov, Nonuniform state of superconductors, *Zh. Eksp. Teor. Fiz.* **47**, 1136 (1964) [*Sov. Phys. JETP* **20**, 762 (1965)].
- [34] Y. Ohashi, On the Fulde-Ferrell State in Spatially Isotropic Superconductors, *J. Phys. Soc. Jpn.* **71**, 2625 (2002).
- [35] S. Uji, T. Terashima, M. Nishimura, Y. Takahide, T. Konoike, K. Enomoto, H. Cui, H. Kobayashi, A. Kobayashi, H. Tanaka, M. Tokumoto, E. S. Choi, T. Tokumoto, D. Graf, and J. S. Brooks, Vortex Dynamics and the Fulde-Ferrell-Larkin-Ovchinnikov State in a Magnetic-Field-Induced Organic Superconductor, *Phys. Rev. Lett.* **97**, 157001 (2006).
- [36] H. Hu and X.-J. Liu, Mean-field phase diagrams of imbalanced Fermi gases near a Feshbach resonance, *Phys. Rev. A* **73**, 051603(R) (2006).
- [37] H. Hu, X.-J. Liu, and P. D. Drummond, Phase Diagram of a Strongly Interacting Polarized Fermi Gas in One Dimension, *Phys. Rev. Lett.* **98**, 070403 (2007).
- [38] D. E. Sheehy, Fulde-Ferrell-Larkin-Ovchinnikov state of two-dimensional imbalanced Fermi gases, *Phys. Rev. A* **92**, 053631 (2015).
- [39] L. He, H. Lü, G. Cao, H. Hu, and X.-J. Liu, Quantum fluctuations in the BCS-BEC crossover of two-dimensional Fermi gases, *Phys. Rev. A* **92**, 023620 (2015).
- [40] C. A. R. Sá de Melo, M. Randeria, and J. R. Engelbrecht, Crossover from BCS to Bose superconductivity: Transition temperature and time-dependent Ginzburg-Landau theory, *Phys. Rev. Lett.* **71**, 3202 (1993).
- [41] X.-J. Liu and H. Hu, BCS-BEC crossover in an asymmetric two-component Fermi gas, *Europhys. Lett.* **75**, 364 (2006).
- [42] J. A. Hertz, Quantum critical phenomena, *Phys. Rev. B* **14**, 1176 (1976).
- [43] A. J. Millis, Effect of a nonzero temperature on quantum critical points in itinerant fermion systems, *Phys. Rev. B* **48**, 7183 (1993).
- [44] H. Hu, Z. Liu, and X.-J. Liu, Unconventional superconductivity of an altermagnetic metal: Polarized BCS and inhomogeneous Fulde-Ferrell-Larkin-Ovchinnikov states, arXiv:2505.0xxxx (2025).
- [45] We have investigated the presence of quantum Lifshitz points in systems with d_{xy} -wave and $d_{x^2-y^2}$ -wave altermagnetism, considering both s -wave and d -wave attractive interactions. These findings indicate that the spin-splitting in the dispersion relation induced by altermagnetism plays the dominant role.
- [46] D. J. Scalapino, E. Loh, Jr., and J. E. Hirsch, d -wave pairing near a spin-density-wave instability, *Phys. Rev. B* **34**, 8190(R) (1986).